

See discussions, stats, and author profiles for this publication at: <https://www.researchgate.net/publication/49780240>

# Effect of the concentration on sol-gel transition of telechelic polyelectrolytes

ARTICLE in THE JOURNAL OF CHEMICAL PHYSICS · JANUARY 2011

Impact Factor: 2.95 · DOI: 10.1063/1.3532090 · Source: PubMed

CITATIONS

5

READS

13

4 AUTHORS, INCLUDING:



Ran Zhang

Chinese Academy of Sciences

12 PUBLICATIONS 41 CITATIONS

SEE PROFILE



Tongfei Shi

Chinese Academy of Sciences

91 PUBLICATIONS 667 CITATIONS

SEE PROFILE



Hongfei Li

Chinese Academy of Sciences

46 PUBLICATIONS 493 CITATIONS

SEE PROFILE

# Effect of the concentration on sol–gel transition of telechelic polyelectrolytes

Ran Zhang,<sup>1,2</sup> Tongfei Shi,<sup>1,a)</sup> Hongfei Li,<sup>1</sup> and Lijia An<sup>1,b)</sup>

<sup>1</sup>State Key Laboratory of Polymer Physics and Chemistry, Changchun Institute of Applied Chemistry, Chinese Academy of Sciences, Changchun 130022, China

<sup>2</sup>Graduate University of the Chinese Academy of Sciences, Beijing 100049, China

(Received 9 August 2010; accepted 6 December 2010; published online 20 January 2011)

Telechelic polyelectrolytes, bearing short hydrophobic blocks at both ends, will ionize into polyions and their counterions when dissolved in water. With the variation of concentration, the interplay between short range attraction and the long range electrostatic interaction as well as the counterion distribution exerts a major influence on the chain conformations (two basic conformations: loop and nonloop, the latter can be subdivided into three association types: free, dangling, and bridge), the cluster structure and the forming of a physical gel. For weak hydrophobic interaction, the relative strong electrostatic interaction dominates the gelation progress; sol–gel transition occurs at higher concentrations due to electrostatic screening and mainly involves the forming of stretched nonloop conformations such as dangling and bridge. While for strong hydrophobic interaction, the hydrophobic interaction dominates and the electrostatic interaction provides a contribution to the formation of gels by maintaining a spatial swelling structure, resulting in a much lower concentration region of sol–gel transition; besides, the sol–gel transition is characterized by the competition of the forming of loop and bridge chains. © 2011 American Institute of Physics. [doi:10.1063/1.3532090]

## I. INTRODUCTION

Physical gels constructed by telechelic polyelectrolytes (TPs) have found many potential applications,<sup>1–7</sup> such as the pharmaceuticals and rheological modifications. As a kind of the telechelic A-B-A polymer, a widely investigated model system, TPs with hydrophobic ends possesses a polyelectrolyte middle block, which has brought interesting but complicated associating behavior.<sup>8–17</sup> The association types of traditional telechelic A-B-A polymer in solution mainly include free, dangling, loop, and bridge, which can be categorized into two main conformations, loop and nonloop.<sup>18</sup> Investigation of the relationship between association types and sol–gel transition in a microscale can be meaningful and helpful for the comprehension of gelation mechanism. However, there are few reports on these of charged telechelic polyelectrolytes. In fact, the TPs could exhibit more complicated relationship than neutral ones when electrostatic interaction is introduced.<sup>19</sup>

The hydrophobic interaction in the short range is an essential factor for the aggregation of telechelic chains into gels. When the middle hydrophilic blocks are replaced by polyelectrolytes, long range electrostatic repulsion originated from the middle block causes the chains more extended, which has an influence on the association behavior and consequently affecting the macroscopic properties.<sup>8–15</sup> Compared with the nonionic telechelics, the gelation of TP is often characterized by a narrower deformation range in the linear viscoelastic regime, a much higher plateau modulus and

lower gelation threshold.<sup>8–15</sup> Moreover, different from the nonionic telechelics, the TPs usually distinguish themselves by a yield stress and several shear-thinning regimes in the flow behavior.<sup>8–10,13,15</sup> In microscale, the association type of chains will also be influenced. At low concentrations, chains will form flowerlike micelles and the chain association type is reported to experience a transition from loop to bridge above a certain concentration, forming a 3D network structure.<sup>10,13</sup> However, the association behavior does not obey this mechanism in some cases when the electrostatic interaction is relatively strong or the middle block has only a few Kuhn segments.<sup>14,15</sup> In theoretical works,<sup>16,17</sup> in dilute solutions, chains tend to form finite size clusters or infinite size gels under certain conditions and the sol–gel transition is depicted as a phase separation; the stabilization mechanism of the associated clusters is found to be related to the attraction of stickers (hydrophobic end groups), coulombic interaction originated from the middle block and the translational entropy of counterions. However, until now there are few systematic investigations on the relationship among the association behavior of chains, aggregation of clusters, and sol–gel transition in polyelectrolytes system. In our previous work, we only present this aspect with the variation of hydrophobic interaction and electrostatic interaction at a fixed concentration, close to the overlapping concentration. For TPs, concentration is another important factor for chain association behavior, which could strongly influence the formation and development of clusters and sol–gel transition. In fact, the increasing concentration of polyelectrolytes leads to not only the increase of polyions dissolved in the solution, but also the more increase of counterions in the system. Furthermore, counterions, to some extent, will screen the electrostatic repulsion between charged monomers, so that the chain structure will be influenced.<sup>20,21</sup>

<sup>a)</sup>Author to whom correspondence should be addressed. Electronic mail: tfshi@ciac.jl.cn. Tel.: +86-431-85262137. FAX: +86-431-85262969.

<sup>b)</sup>Electronic mail: ljan@ciac.jl.cn.

Therefore, concentration is an important factor for the gelation behavior of TP which can not be ignored.

In this paper, we will investigate the chain conformation, development and inner structure of clusters during the process of gelation through the variation of concentrations at different hydrophobic interaction. It is found that with the increase of concentration the interplay between short range hydrophobic attraction and long range electrostatic repulsion has a major influence on the gelation behavior of TPs. The Monte Carlo method we use is described in Sec. II, followed by the simulation results and discussion. Our conclusions will be drawn in Sec. IV.

## II. MODEL AND SIMULATION DETAILS

An off-lattice Monte Carlo simulation is performed to investigate the TPs. In a cubic cell ( $L = 48\sigma$ ) with periodic boundary conditions in 3 dimensions, the TP chain has a structure  $A_{N_A} - B_{N_B} - A_{N_A}$  containing 20 monomers, with  $N_A \equiv 1$  and  $N_B \equiv 18$ . Block A stands for the hydrophobic groups, and block B is a flexible hydrophilic polyelectrolyte, fully charged, bond length is fixed at  $1.1\sigma$ . Polyelectrolyte monomers and their counterions are monovalent and carrying negative and positive charges, respectively. The number of counterions equals to the number of polyelectrolyte monomers to maintain the charge neutrality. The solvent is implicitly treated as a dielectric continuum. No salt is added. The simulation work is done in the NVT (constant particle numbers, constant volume and temperature) ensemble according to the Metropolis algorithm. There would be at most 240 chains in the simulation box and several algorithms were used to relax the TP chains.<sup>19</sup> The attraction potential between hydrophobic monomers  $U_{attr}$  is an attractive Lennard-Jones potential:

$$U_{attr} = 4\varepsilon_{attr} \left[ \left( \frac{\sigma_{attr}}{r} \right)^{12} - \left( \frac{\sigma_{attr}}{r} \right)^6 \right], \quad (1)$$

where  $\varepsilon_{attr}$  is the association energy. The interaction between other pairs is represented by the repulsive L-J potential:

$$U_{rep} = 4\varepsilon_{rep} \left( \frac{\sigma_{rep}}{r} \right)^{12}, \quad (2)$$

where  $\varepsilon_{rep}$  is the repulsive energy and fixed at  $0.5k_B T$ . Here  $\sigma_{attr} = \sigma_{rep} = \sigma = 1$  and the cutoffs of these L-J interactions is  $2.5\sigma$ . According to Ewald method, the expression of Coulomb potential  $U_{elec,tot}$  is

$$U_{elec,tot} = k_B T \lambda_B E_{tot}, \quad (3)$$

$$E_{tot} = E_r + E_k + E_s + E_d, \quad (4)$$

where  $k_B$  is the Boltzmann constant,  $T$  refers to temperature, the Bjerrum length  $\lambda_B$  ( $\lambda_B = e^2/4\pi\varepsilon_o\varepsilon_r k_B T$ ) is defined as the distance at which two unit charges have the interaction energy  $k_B T$ . Here,  $\lambda_B$  can be considered as a measure of the strength of electrostatic interactions versus the thermal energy and is equal to  $7.14 \text{ \AA}$  for water at room temperature. Here,  $e$  is the elementary unit charge;  $\varepsilon_o$  and  $\varepsilon_r$  are the relative dielectric constants of the vacuum and the solvent(water), respectively.

The coulombic strength  $\xi$  ( $\xi = \lambda_B/\sigma$ ) is set at 0.5 for simplicity. Here,  $E_r$  and  $E_k$  on the right of Eq. (4) are the contributions from the real space and the Fourier space,  $E_s$  is the self-term and  $E_d$  is the dipole-correction term.<sup>22</sup> These potentials are

$$E_r = \frac{1}{2} \sum_{i,j} \sum_{\vec{n}} q_i q_j \frac{\text{erfc}(\alpha|r_{ij} + \vec{n}L|)}{|r_{ij} + \vec{n}L|}, \quad (5)$$

$$E_k = \frac{1}{2} \frac{1}{\pi L^3} \sum_{\vec{k} \neq 0} \frac{4\pi^2}{k^2} \exp\left(-\frac{k^2}{4\alpha^2}\right) |\tilde{\rho}(\vec{k})|^2, \quad (6)$$

$$E_s = -\frac{\alpha}{\sqrt{\pi}} \sum_{i=1}^N q_i^2, \quad (7)$$

$$E_d = \frac{2\pi}{(1 + 2\varepsilon_s)L^3} \left| \sum_{i=1}^N q_i \vec{r}_i \right|^2. \quad (8)$$

In Eq. (6) the reciprocal vector  $\vec{k} = 2\pi\vec{n}/L$ ,  $\vec{n} = (n_1, n_2, n_3)$ :  $n_i \in \mathbb{Z}$ . In Eq. (8)  $\varepsilon_s$  is the dielectric constant of the medium surrounding the sphere.<sup>22</sup> How to manipulate the Coulomb sum using a Monte Carlo style is thoroughly discussed in the former paper and here the measure we take is exactly the same.

## III. SIMULATION RESULTS

### A. Gelation process

For TPs, increasing hydrophobic interaction may lead to a transition from sol to gel at a fixed concentration, which has been investigated in our previous work.<sup>19</sup> If the hydrophobic interaction is fixed, increasing concentration can also leads to a transition from sol to gel. However, the gelation behavior originated from the variation of hydrophobic interaction at fixed concentration may be different from that from the variation of concentration at fixed hydrophobic interaction. In addition, for different hydrophobic interaction, the effect of concentration on gelation could be different. In theoretical studies of TP,<sup>16,17</sup> usually the minimization of free energy is employed to determine the forming of clusters or a gel; here we choose percolation theory<sup>23,24</sup> model because it is convenient to judge the sol-gel transition in our Monte Carlo simulation, and the criteria for determining the sol-gel transition by percolation theory that  $\varepsilon_{attr}$  is much higher than  $k_B T$  are met in this work.<sup>25,26</sup> Here, a dimensionless variable  $\varepsilon$  is introduced to control the hydrophobic interaction,  $\varepsilon = \varepsilon_{attr}/k_B T$ . Figure 1 plots the percolation values against concentration  $\phi$  at different  $\varepsilon$ . When the percolation value  $P(\phi, \varepsilon) = 0$ , the system is in the sol state; with the increasing of  $\phi$ ,  $P(\phi, \varepsilon)$  shows an abrupt slope and reaches 1; after that, the system is in a gel state; the concentration area between the two states can be viewed as a sol-gel transition region. The solid lines are Sigmoidal-Boltzmann fitting curves to the percolation data points. The sol-gel transition concentration range can be roughly acquired, such as  $0.028 < \phi < 0.04$ ,  $0.014 < \phi < 0.024$ , and  $0.013 < \phi < 0.018$  for  $\varepsilon = 5, 7$ , and  $8$ , respectively. It is found that

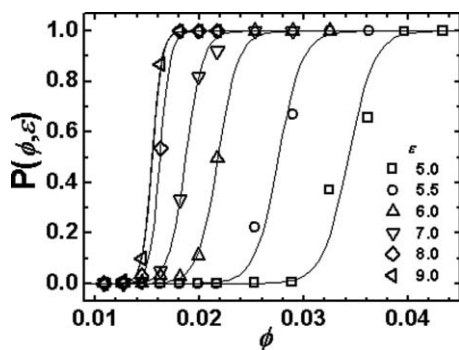


FIG. 1. (a) Percolation probability plotted against concentration  $\phi$  at different hydrophobic interaction energy  $\varepsilon$ . The solid line is the Sigmoidal-Boltzmann fit of the percolation data.

when  $\varepsilon$  increases, the sol-gel transition shifts to lower concentration area and the sol-gel transition region gets narrower. This is because the sol-gel transition region at higher  $\varepsilon$  (such as  $\varepsilon = 8$  and  $\varepsilon = 9$ ) covers the overlapping concentration  $\phi^*$  ( $\phi^* \approx 0.016$ , acquired by viewing the whole chain as a linear polyelectrolyte in water), and gelation cannot form at concentrations lower than overlapping concentration. However, in earlier works of TP, Potemkin *et al.*<sup>16</sup> proposed a stabilizing phase of finite size cluster, describing clusters formed with an inner network of connected chains, which has a maximum in size distribution function, and Zaroslov *et al.*<sup>27</sup> found that this concept is a better approximation of their (PS)<sub>2</sub>PMANa particles formed in aqueous media.

## B. Chain association types

As we know, there are two conformations in TP, which can be further divided into four main association types of chain, free, loop, dangling, and bridge (see Fig. 2).<sup>19</sup> Experimentally,<sup>8–15,27</sup> the probable chain type or the transition between different types can only be deduced by scattering methods, rheological techniques, or spectroscopy studies; as for theoretical studies,<sup>16,17,28</sup> further information of the chain conformations is rarely reported. To further understand the sol-gel transition with the variation of concentration,

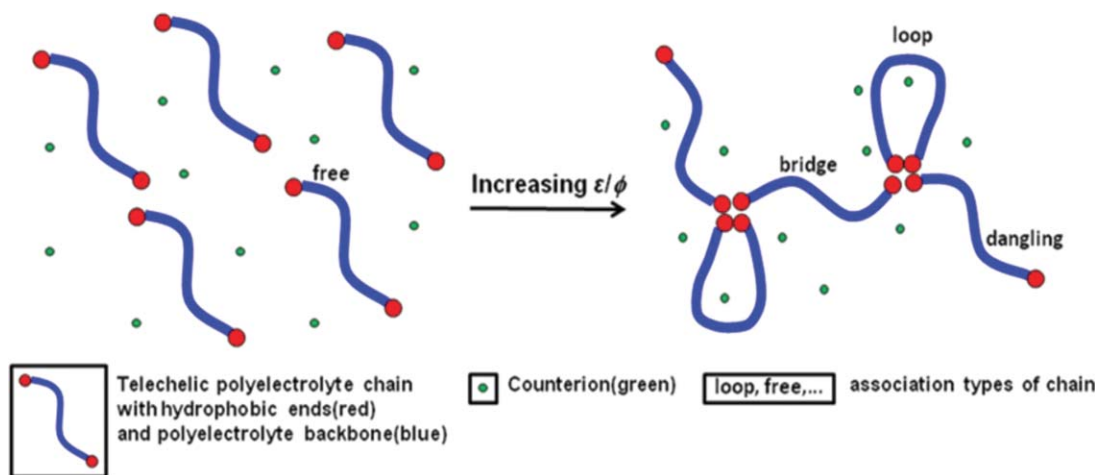


FIG. 2. Sketch map of telechelic polymers in aqueous solution, illustrating the concept of chain association types.

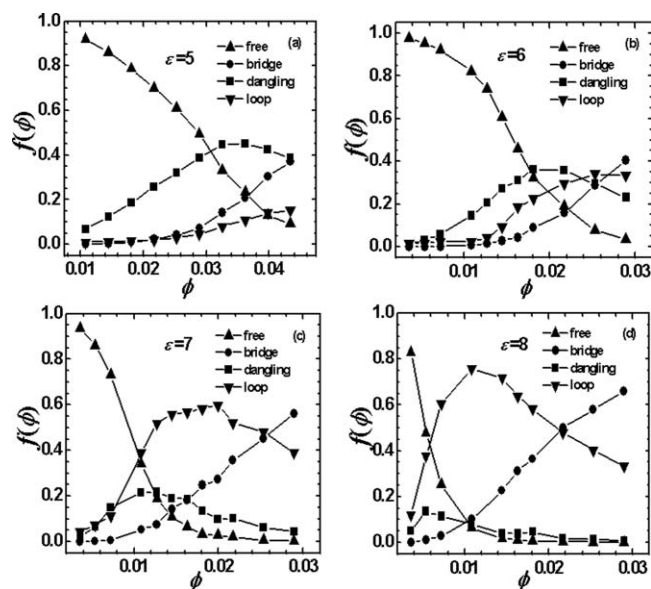


FIG. 3. The fraction of chain association type as a function of concentration at different interaction energy  $\varepsilon$ . From (a) to (d),  $\varepsilon = 5, 6, 7$ , and  $8$ , respectively.

the contributions of different association types to the formation of gel are investigated here. Figure 3 shows the fraction of different types of association  $f(t, \phi)$  versus concentration  $\phi$  at different hydrophobic conditions. At very low concentration, the TP chains are stretched and most of them maintain a free type.  $f(\text{free}, \phi)$  decreases with increasing  $\phi$  and this decreasing trend gets more pronounced with the increase of hydrophobic interaction  $\varepsilon$ . This is because increasing  $\phi$  makes for the aggregation of the interchain hydrophobic ends. Dangling chains are considered as an intermediate here, namely free chains can form danglings and some of danglings can change into other types like loop or bridge. Therefore, there exists a competition between the forming and consuming of dangling chains, causing a maximum of  $f(\text{dangling}, \phi)$  with increasing  $\phi$ . Moreover, from Figs. 3(a) to 3(d), with increasing hydrophobic interaction, the concentration where the maximum of  $f(\text{dangling}, \phi)$  is reached shifts to a



lower concentration, and the value of the maximum becomes smaller. This is because increasing hydrophobic interaction favors the transition of dangling chains to bridge and loop chains.

Compared with  $f(\text{bridge}, \phi)$ ,  $f(\text{loop}, \phi)$  shows quite a different developing process with  $\phi$  at different  $\varepsilon$ . In Figure 3(a),  $f(\text{loop}, \phi)$  and  $f(\text{bridge}, \phi)$  at lower  $\phi$  show no increase until  $\phi > 0.025$ . This is because the hydrophobic interaction is relatively weak in the competition with the repulsive electrostatic interaction. Thus, the backfolding of TP chains and the forming of interchain hydrophobic aggregation are not favorable at low concentration. In this case, chains are found to form loose aggregates like starlike micelles.<sup>14</sup> However, further increasing concentration will lead to the electrostatic interaction screened,<sup>20,21</sup> which will favor the backfolding and interchain aggregation. Furthermore, in the gel state, the  $f(\text{loop}, \phi)$  value is not more than 0.15 and  $f(\text{bridge}, \phi)$  is less than 0.4, suggesting the forming of bridges is more favorable than the forming of loops at higher concentration and the aggregation behavior is greatly reduced by the comparatively strong electrostatic repulsions.

Obviously, from Figs. 3(a) to 3(d), increasing hydrophobic interaction favors the formation of bridge chains due to larger fraction of  $f(\text{bridge}, \phi)$  at higher  $\varepsilon$ . Moreover, at different hydrophobic interaction, the tendency of  $f(\text{bridge}, \phi)$  versus  $\phi$  shows a similar increasing pattern, implying that the bridge chains are favorable with increasing  $\phi$ . However, the tendency of  $f(\text{loop}, \phi)$  versus concentration is different at different hydrophobic interaction. Compared with  $f(\text{loop}, \phi)$  at  $\varepsilon = 5$  [see Fig. 3(a)],  $f(\text{loop}, \phi)$  at  $\varepsilon = 7$  increases sharply in the sol state ( $\phi < 0.014$ ) and then reaches a maximum (about 0.6) at  $\phi \approx 0.02$  in the sol–gel region and finally shows a decrease [see Fig. 3(c)]. When  $\varepsilon = 8$ ,  $f(\text{loop}, \phi)$  increases more significantly compared with that at  $\varepsilon = 7$  and reaches a maximum (about 0.75) at  $\phi \approx 0.011$  in sol region. This indicates that stronger hydrophobic interaction favors the formation of loop chains at lower concentration. However, a further increase of  $\phi$  leads to more probability of the aggregation of interchain hydrophobic groups; moreover, the forming of loops will accumulate the repulsive electrostatic energy, which hinders the other stretched chains to fold back. On the other hand, bridges are favorable with increasing  $\phi$  and stronger  $\varepsilon$ , since the forming of bridges can balance the electrostatic repulsion and the hydrophobic attraction. The competition between the forming of loops and bridges induces  $f(\text{loop}, \phi)$  to decrease after reaching the maximum. In addition, Fig. 3(d) shows that during the sol–gel transition chains are mainly composed of the loop and bridge chains and  $f(\text{loop}, \phi)$  decreases and  $f(\text{bridge}, \phi)$  increases with increasing  $\phi$ , indicating a loop to nonloop conformation transition, which coincides with the experimental results,<sup>10,13,27</sup> while in Fig. 3(a) the sol–gel transition involves mainly the transition of association types in the non-loop conformation due to relative small variation of  $f(\text{loop}, \phi)$  with concentration during the sol–gel transition.

During the sol–gel transition, the averaged  $R_G$  of TP chains gives a new insight of TP gelation, since in experimental studies,<sup>27</sup> the size of clusters instead of the size of a single chain is often provided as a characterization method. In simulation, an investigation of  $R_G$  can be helpful for our

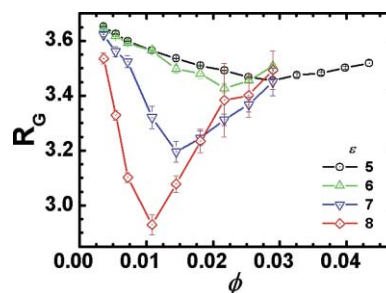


FIG. 4. The radius of gyration  $R_G$  plotted against  $\phi$  at different  $\varepsilon$ .

understanding of polymer structure in microscale. The radius of gyration,  $R_G$ , of TP chains plotted against  $\phi$  is shown in Fig. 4. It is found that the stronger the hydrophobic interaction, the larger is variation of  $R_G$  values with  $\phi$ . When  $\varepsilon = 8$ , the  $R_G$  decreases sharply as  $\phi$  increases and reaches a minimum of about 2.92 at  $\phi = 0.011$ , which is consistent with the concentration location of the maximum point of  $f(\text{loop}, \phi)$  in Fig. 3(d). After the minimum,  $R_G$  gives a quick increase with increasing  $\phi$ . The trend of  $R_G$  clearly corresponds to the  $f(\text{loop}, \phi)$  in a reverse way. When the hydrophobic interaction is very weak, e.g.,  $\varepsilon = 5$ ,  $R_G$  shows a slow decrease as  $\phi$  increases from about 3.65 to 3.45, due to the screening effects caused by the increasing  $\phi$ ; as  $\phi$  gets higher,  $R_G$  does not keep on decreasing but gives a slight increase and reaches around 3.52. This is because relatively strong electrostatic repulsion causes most chains to maintain a nonloop conformation and the forming of bridges among micelles stretches the telechelic chain. Loop conformation, on the other hand, is not favored under this condition and has no significant influence on  $R_G$ . As for relative intermediate hydrophobic interactions ( $\varepsilon = 6$  and 7), when  $\varepsilon$  decreases, the minimum value of  $R_G$  increases and the concentration locating the minimum shifts to a higher area. Their  $R_G$  curves act as a transition from  $\varepsilon = 5$  to  $\varepsilon = 8$ .

### C. Clusters and gelation mechanisms

Basically, with the increase of concentration, clusters are connected together by bridge chains to form a spatial structure; above some percolation threshold, a 3D network in the system is formed. Potemkin *et al.*<sup>16,17</sup> proposed the microgels formed during the TP gelation process, these microgels are described as clusters with inner netlike structure and has maximum size of distribution, which is proved by Zaroslov *et al.*<sup>27</sup> However, increasing concentration at different hydrophobic interactions strongly influences the association behavior according to the above discussion on chain associations. As a result, the variation of the association behavior of chains will affect the formation and development of clusters and even their inner structure. To investigate the cluster development and, more important, their inner structure with concentration at different hydrophobic interactions will be helpful for understanding the gelation mechanism. However, there are few systematic discussions.

Figure 5 shows the development of cluster size distribution with increasing  $\phi$ . When the hydrophobic interaction is very strong [ $\varepsilon = 8$ , see Fig. 5(a)], it is obvious that clusters

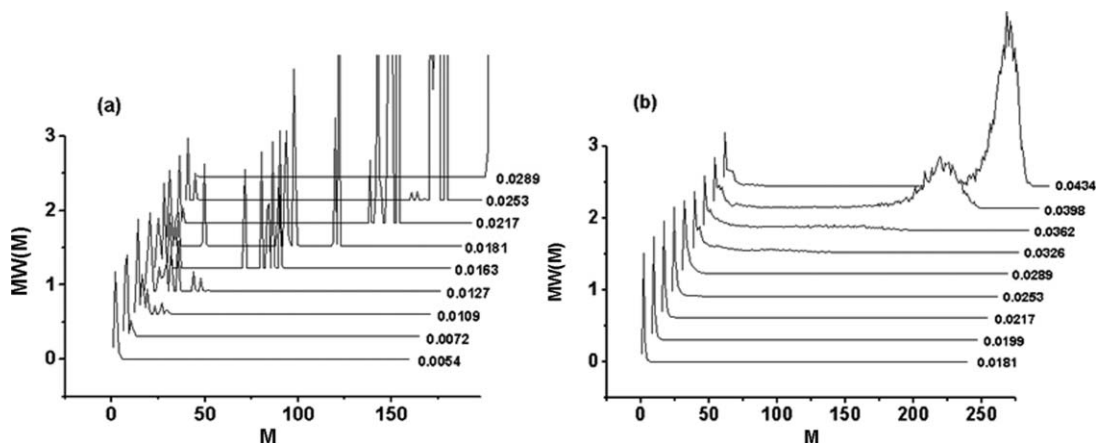


FIG. 5. Distribution of clusters at different concentrations, (a)  $\varepsilon = 8$ ; (b)  $\varepsilon = 5$ . The cluster distribution function  $W(M) = N(M)/[N(1)+N(2)+\dots+N(N)]$ ,  $N(M)$  is the number of clusters of size  $M$ .

grow with concentration in the sol state; the cluster size in the sol-gel region ( $0.013 < \phi < 0.018$ ) has a trend to form two extreme distributions: very large and very small, and this feature is more obvious in the gel state ( $\phi > 0.018$ ). These indicate that aggregation of chains is prevailing with increasing  $\phi$ . At the same concentration, however, the cluster distribution of neutral telechelics is completely different. For instance, in Fig. 6(a), at  $\phi = 0.0289$ , a peak at very large cluster size suggests a gel state for the TPs, while a broad distribution of the cluster size indicates the sol-gel state for the neutral telechelics. It is obvious that for strong hydrophobic interaction, the electrostatic interaction provides a contribution to the formation of gels by maintaining a spatial swelling structure. Without the support of electrostatic repulsion, the size of chain ( $R_G$ ) gets smaller and a continuous network could be broken.<sup>19</sup> Figure 7(a) shows that the chains will form flowerlike micelles in the sol state as Fig. 3(d) implies; with the increase of  $\phi$ , these micelles are further connected by bridges to form large clusters, and the loop conformation are not favored, the forming of bridges are prevailing, resulting in larger clusters with narrow distributions. When entering the sol-gel transition, these clusters start to present a distribution of two extreme sizes. Moreover, the sol-gel transition involves the competition between the forming of loops and bridges, resulting in a loop to nonloop conformation transition through gelation process.<sup>10,13</sup> Snapshots

of simulation in Figs. 7(b) and 7(c) illustrate the loop to nonloop conformation transition during the gelation process. Figure 7(b) shows the cluster inner structure containing several loop chain, which can be viewed as an aggregation of flowerlike micelles in Fig. 7(a); with increasing  $\phi$  the gel network develops complete, Fig. 7(c) actually shows a small part of the network, where bridges are prevailing instead of loops.

In Figure 5(b), when the hydrophobic interaction is weaker ( $\varepsilon = 5$ ), the size of clusters grows very slowly with concentration in the sol state, which implies the aggregation of chains is unfavorable compared with that at strong hydrophobic interactions; the hydrophobic blocks aggregate with the help of screened electrostatic interaction as  $\phi$  increases, causing a wide and smooth distribution of the cluster size in the sol-gel transition area ( $0.028 < \phi < 0.04$ ); when the system is in the gel state, the clusters begin to take on a look of two distribution sizes and the peaks are much broader than that at  $\varepsilon = 8$  in Fig. 5(a). For neutral telechelics without the electrostatic interactions, the aggregation of chains is much favorable. Figure 6(b) shows that in the sol-gel state, the cluster size distribution of TPs is wide and smooth distribution, while the cluster size distribution of neutral telechelics is a series of narrow peaks. It is obvious that for weaker hydrophobic interaction, the relative strong electrostatic interaction dominates in the formation of gels, which causes the aggregation of chains unfavorable. Therefore, in

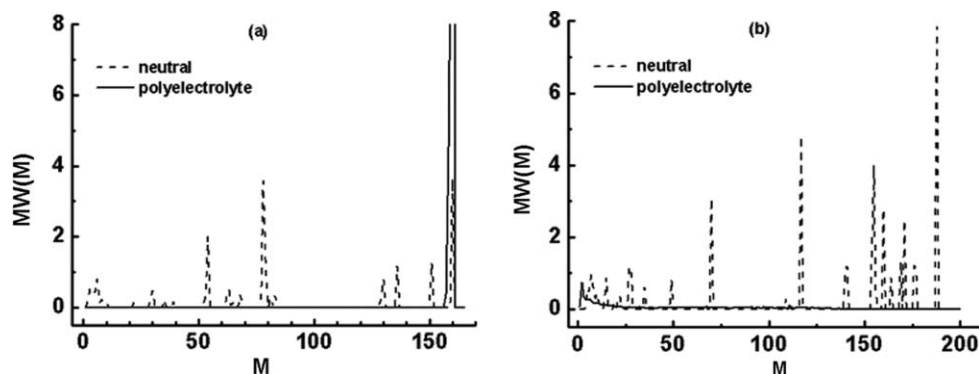


FIG. 6. Distribution of clusters of neutral telechelics and telechelic polyelectrolytes. (a)  $\phi = 0.0289$ ,  $\varepsilon = 8$ ; (b)  $\phi = 0.0362$ ,  $\varepsilon = 5$ .

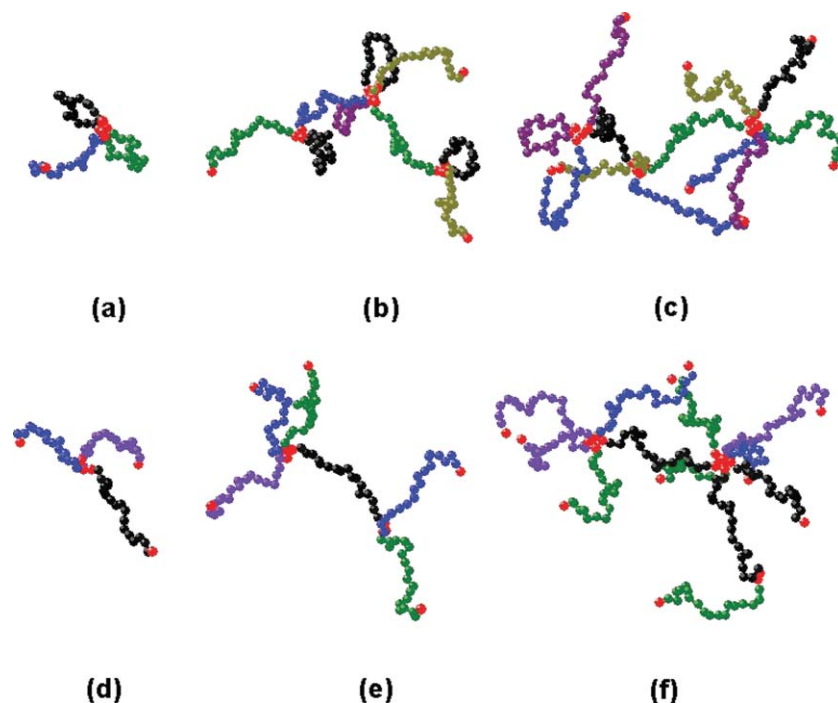


FIG. 7. Snapshots during the simulation showing development of clusters. (a)  $\phi = 0.0072$ ,  $\varepsilon = 8$ ; (b)  $\phi = 0.0145$ ,  $\varepsilon = 8$ ; (c)  $\phi = 0.0289$ ,  $\varepsilon = 8$ ; (d)  $\phi = 0.0145$ ,  $\varepsilon = 5$ ; (e)  $\phi = 0.0217$ ,  $\varepsilon = 5$ ; (f)  $\phi = 0.0362$ ,  $\varepsilon = 5$ . Hydrophobic end blocks are shown in red color. As a guide to the eye, different colors are used for the middle polyelectrolyte blocks. Counterions and some of the chains are omitted to acquire a better view of cluster structure.

sol state, the fraction of bridge and loop chains are very low and chains are mainly composed of dangling and free chains. Thus, the micelles are starlike rather than flowerlike [see Fig. 7(d)]. Increasing concentration will cause screening to the electrostatic interaction, which is helpful for the aggregation of chains. Thus, the starlike micelles are bridged to form clusters, which could be described as dendritic aggregation. The dendritic cluster shape is well represented by Figs. 7(e) and 7(f). However, with the background of relative weak hydrophobic interaction, it is insufficient to fold back the chain to form a loop. The forming of loops under this condition is triggered by increasing  $\phi$  and screened electrostatic repulsion. Thus, the sol–gel transition involves the forming of clusters characterized mostly by nonloop chains as danglings and bridges with the help of screened electrostatic interaction as  $\phi$  increases, but only a few chains change into loop conformation. It is obvious that increasing concentration can screen electrostatic repulsion in some degree, but the relative strong electrostatic repulsion has a disadvantage to the aggregation of chains, which will arouse a wide distribution of cluster size even in gel state.

#### IV. CONCLUSION

In our previous work, the effect of the interplay of hydrophobic interaction and electrostatic interaction on physical gelation of TP has been investigated. In this work, we focus on the concentration effect. It is obvious that the two gelation behaviors are different. As for weaker hydrophobic interaction, the relative strong electrostatic interaction dominates the gelation progress. The relative strong electrostatic repulsion has disadvantages to the chain aggregation;

however, increasing concentration can screen electrostatic repulsion in some degree, which makes for the growth of clusters and the sol–gel transition; when the gelation progress is completed, although there are two extremes in the distribution of cluster size, a relative wide peak of cluster size distribution in large cluster region indicates that the strong electrostatic repulsion still affects the aggregation. Sol–gel transition mainly involves the change of dangling to bridge due to very low fraction of the loop chains. However, as for strong hydrophobic interaction, the hydrophobic interaction dominates and electrostatic interaction provides a contribution to the formation of gels by maintaining a spatial swelling structure. Sol–gel transition involves the competition of loop and bridge chains, which includes a loop to nonloop (mainly bridge chains) conformation transition. In the gel state, a very narrow peak of cluster size distribution in large cluster region indicates that hydrophobic interaction still dominates so the chain aggregation is favorable. Furthermore, in our previous work, the gelation with the variation of the hydrophobic interaction is much complicated and different from that with the variation of concentration in this work. In fact, it undergoes a transition from the electrostatic interaction domination to the hydrophobic interaction domination. Of course, the salt concentration is also a very important factor for the gelation of TP, which will be in our future work.

#### ACKNOWLEDGMENTS

This work is supported by the National Natural Science Foundation of China (20734003, 20774096) Programs and the Fund for Creative Research Groups (50921062); T.F.S. thanks the supports from the Special Funds for National Basic Research Program of China (2009CB930100).

- <sup>1</sup>A. Serres, M. Baudys, and S. W. Kim, *Pharm. Res.* **13**, 196 (1996).
- <sup>2</sup>L. E. Bromberg and E. S. Ron, *Adv. Drug Delivery Rev.* **31**, 197 (1998).
- <sup>3</sup>S. H. Yuk and Y. H. Bae, *Crit. Rev. Ther. Drug Carrier Syst.* **16**, 385 (1999).
- <sup>4</sup>Y. Qiu and K. Park, *Adv. Drug Delivery Rev.* **53**, 321 (2001).
- <sup>5</sup>A. Wittemann, T. Azzam, and A. Eisenberg, *Langmuir* **23**, 2224 (2007).
- <sup>6</sup>I. C. Riegel, D. Samios, C. L. Petzhold, and A. Eisenberg, *Polymer* **44**, 2117 (2003).
- <sup>7</sup>C. L. He, S. W. Kim, and D. S. Lee, *J. Controlled Release* **127**, 189 (2008).
- <sup>8</sup>C. Tsitsilianis, I. Iliopoulos, and G. Ducouret, *Macromolecules* **33**, 2936 (2000).
- <sup>9</sup>C. Tsitsilianis, I. Katsampas, and V. Sfika, *Macromolecules* **33**, 9054 (2000).
- <sup>10</sup>I. Katsampas and C. Tsitsilianis, *Macromolecules* **38**, 1307 (2005).
- <sup>11</sup>C. Tsitsilianis and I. Iliopoulos, *Macromolecules* **35**, 3662 (2002).
- <sup>12</sup>C. Esquenet, P. Terech, F. Boue, and E. Buhler, *Langmuir* **20**, 3583 (2004).
- <sup>13</sup>N. Stavrouli, T. Aubry, and C. Tsitsilianis, *Polymer* **49**, 1249 (2008).
- <sup>14</sup>G. T. Gotzamanis, C. Tsitsilianis, S. C. Hadjiyannakou, C. S. Patrickios, R. Lupitsky, and S. Minko, *Macromolecules* **39**, 678 (2006).
- <sup>15</sup>F. Bossard, T. Aubry, G. Gotzamanis, and C. Tsitsilianis, *Soft Matter* **2**, 510 (2006).
- <sup>16</sup>I. I. Potemkin, V. V. Vasilevskaya, and A. R. Khokhlov, *J. Chem. Phys.* **111**, 2809 (1999).
- <sup>17</sup>I. I. Potemkin, S. A. Andreenko, and A. R. Khokhlov, *J. Chem. Phys.* **115**, 4862 (2001).
- <sup>18</sup>F. Tanaka, *J. Non-Cryst. Solids* **307**, 688 (2002).
- <sup>19</sup>R. Zhang, T. F. Shi, and L. J. An, *J. Phys. Chem. B* **114**, 3449 (2010).
- <sup>20</sup>M. J. Stevens and K. Kremer, *J. Chem. Phys.* **103**, 1669 (1995).
- <sup>21</sup>R. G. Winkler, M. Gold, and P. Reineker, *Phys. Rev. Lett.* **80**, 3731 (1998).
- <sup>22</sup>M. P. Allen and D. J. Tildesley, *Computer Simulations of Liquids* (Oxford University Press, London, 1987).
- <sup>23</sup>D. Stauffer and A. Aharony, *Introduction to Percolation Theory* (Taylor & Francis, London, 1992).
- <sup>24</sup>G. Ódor G, *Rev. Mod. Phys.* **76**, 663 (2004).
- <sup>25</sup>S. K. Kumar and A. Z. Panagiotopoulos, *Phys. Rev. Lett.* **82**, 5060 (1999).
- <sup>26</sup>S. K. Kumar and J. F. Douglas, *Phys. Rev. Lett.* **87**, 188301 (2001).
- <sup>27</sup>Y. D. Zaroslov, G. Fytas, M. Pitsikalis, N. Hadjichristidis, O. E. Philippova, and A. R. Khokhlov, *Macromol. Chem. Phys.* **206**, 173 (2005).
- <sup>28</sup>R. E. Limberger, I. I. Potemkin, and A. R. Khokhlov, *J. Chem. Phys.* **119**, 12023 (2003).